Enhanced ferroelectric and pyroelectric properties of poly(vinylidene fluoride) with addition of graphene oxides

Cite as: J. Appl. Phys. **115**, 204101 (2014); https://doi.org/10.1063/1.4878935
Submitted: 17 April 2014 . Accepted: 08 May 2014 . Published Online: 23 May 2014

Z. Y. Jiang, G. P. Zheng, Z. Han, Y. Z. Liu, and J. H. Yang

Enhanced ferroelectric and pyroelectric properties of poly(vinylidene fluoride) with addition of graphene oxides

Z. Y. Jiang,[1] G. P. Zheng,[1,a)] Z. Han,[1,2] Y. Z. Liu,[1] and J. H. Yang[2]
[1]*Department of Mechanical Engineering and Shenzhen Research Institute, Hong Kong Polytechnic University, Hung Hom, Kowloon, Hong Kong, China*
[2]*School of Materials Science and Engineering, University of Shanghai for Science and Technology, Shanghai 200093, China*

(Received 17 April 2014; accepted 8 May 2014; published online 23 May 2014)

Poly(vinylidene fluoride)/graphene oxide (PVDF/GO) nanocomposites are synthesized and their structural, ferroelectric, and pyroelectric properties are investigated. The dielectric spectrum analysis and P-E loop tests indicate that the nanocomposites exhibit enhanced ferroelectric and pyroelectric properties compared with those of poly(vinylidene fluoride) samples. The isothermal crystallization kinetics of PVDF/GO nanocomposites quantitatively determined by differential scanning calorimetry demonstrates that GOs facilitate the crystallization of the PVDF. Dynamic mechanical analyses on the PVDF/GO reveal that the amorphous and crystalline phases of PVDF are modified by the addition of GO sheets. The GO-enhanced formation of crystalline β phase in PVDF could result from the strong interaction between the –C = O groups in GO and the $–CF_2$ groups in PVDF, and the GO-induced ordering of the microstructures of amorphous and crystalline phases. The results suggest that PVDF/GO nanocomposites could be promising dielectric materials used in sensors, transducers, and actuators. © *2014 AIP Publishing LLC*. [http://dx.doi.org/10.1063/1.4878935]

I. INTRODUCTION

In the past decades, poly(vinylidene fluoride) (PVDF) has been widely used as functional or structural materials since PVDF has excellent chemical resistance and thermal stability, good mechanical properties and is easy to be processed.[1–6] In particular, PVDF can be used as sensors, transducers, and actuators because of its excellent piezoelectric, pyroelectric, and ferroelectric properties.[7–9] PVDF is a typical semi-crystalline polymer with various amorphous and crystalline phases. PVDF samples usually possess microstructures of amorphous structures and crystalline structures with polar and non-polar phases. The piezoelectric and pyroelectric applications of PVDF are restricted by the difficulties in controlling the microstructure of its polar crystalline β phase. In the β-phase conformation of PVDF, the fluorine and hydrogen atoms are on opposite sides of the polymer backbone, hence the net non-zero dipole moments are formed.[10,11] The presence of these dipoles is what makes PVDF a good piezo- and pyroelectrically active polymer. However, the desirable content of polar crystalline β phase has to be made through mechanical deformation or electrical polling.

In the past several years, nanocomposites consisting of PVDF and graphene or graphene oxides (GOs) are of much interest.[12–15] Although a lot of investigations have been focused on the chemical, mechanical, and dielectric properties of these nanocomposites, the effects of GO blending on the ferroelectric, pyroelectric properties and the microstructures of PVDF are still under debate.[14,15] Recently, El Achaby *et al*. reported that the addition of graphene oxides enhanced the formation of the β phase of PVDF and improved its ferroelectric properties.[13] It was suggested that the strong interaction between the –C = O in GO and $–CF_2$ in PVDF could facilitate the formation of β phase of PVDF.

In this work, we illustrate the enhanced pyroelectric and ferroelectric properties of the nanocomposite consisting of PVDF and GO via different characterization methods. The dielectric spectrum analysis and P-E loop tests are used to investigate the ferroelectric and pyroelectric properties of PVDF-GO nanocomposite. Dynamic mechanical analyses on the PVDF-GO are employed to characterize the amorphous and crystalline structures of PVDF, which are modified by the additive GO sheets. The microstructures of PVDF-GO nanocomposites are further analyzed via the isothermal crystallization kinetics, which is quantitatively determined by differential scanning calorimetry. How the PVDF and graphene oxides affect with each other and contribute to the ferroelectric and pyroelectric properties of the nanocomposites are discussed.

II. EXPERIMENTAL METHODS

A modified Hummers method[16,17] was used to prepare the graphene oxides from natural graphite. The natural graphite powders and sodium nitrates were dissolved in the concentrated sulfuric acid to oxidize the graphite. Then, the solution was stirred in a cold bath for 25 min and potassium permanganate was slowly added to the solution. The solution was kept for another 25 min. Subsequently, the solution was kept at 35 °C for 45 min and the de-ionized water was added to it. After dilution, the H_2O_2 (30%) was added to the solution. The mixture was then processed by filtering, washing, centrifuging, and drying. The graphite oxide was prepared and dissolved in the de-ionized water under sonication for 2 h. After centrifugation, the GO suspension was obtained.

a)E-mail: mmzheng@polyu.edu.hk

The suspension was dried at 60 °C in a vacuum oven till the GO flake was prepared. The GO flake was used for further experiments.

To investigate the potential ferroelectric properties of GOs, the film sample of GOs was prepared on the indium-tin-oxide (ITO) glass substrate. The GO flakes (60 mg) were dispersed in 40 ml de-ionized water and then casted on the ITO glass. The sample was then dried at 70 °C for 24 h to form the GO films (~2 μm in thickness). Gold electrodes with a diameter of 0.1 mm were deposited on the film surface via the magnetron sputtering. The bulk PVDF-GO discs were prepared by the hot press processing method,[18] as follows: First, the graphene oxides (60 mg) were dissolved in N,N-dimethylformamide (DMF) with the assistance of sonication and agitation. Then, the PVDF powders were added to the suspension. The mass ratio of PVDF to GO is 60:1. The suspension was then stirred for 4 h and was dried at 70 °C for 72 h in a vacuum oven to evaporate DMF. The obtained PVDF-GO nanocomposites were subjected to a hot press at 170 °C for 2 h to form the PVDF-GO discs with a diameter of 25 mm and a thickness of 0.6 mm.

The PVDF-GO and PVDF samples with a thickness of 0.6 mm and a diameter of 3.5 mm were cut from the sample discs processed by the hot-pressing method. Silver paste is coated on their top and bottom surfaces as electrodes for dielectric spectrum and P-E loop measurements. The ferroelectric test system (TF2000E, aixACCT) was used to measure the ferroelectric and pyroelectric properties of the samples. The relative permittivity (ε_r) and loss tangent ($\tan\delta$) of these samples were measured at different frequencies using an impedance analyzer (HP 4192A) at 30 °C. Anelastic behaviors of the samples were characterized using a Dynamic Mechanical Analyzer, TA Instruments Q800. The samples with dimensions of 25 mm × 2 mm × 0.5 mm were tested in a tensile mode of dynamic mechanical analysis (DMA). X-ray diffraction (XRD) patterns of the samples were taken by a Philips PW3040/60 X-ray diffractometer with nickel filtered Cu Kα radiation.

III. RESULTS AND DISCUSSION

A. Characterizations

The Raman spectra of GO and PVDF-GO are shown in Fig. 1(a). For GO sample, the D-band and G-band appear at 1340 cm^{-1} and 1580 cm^{-1}, which are caused by the in-plane vibration of graphite with an E_{2g}-symmetry intra-layer mode and the defects in the graphene or amorphous carbon, respectively. The Raman spectrum of PVDF-GO also shows D-band (1329 cm^{-1}) and G-band (1581 cm^{-1}) but the intensity ratio of G-band to D-bands (I_G/I_D) is much higher than that of GO. Between the G-band and D-band, the peak (around Raman shift 1430 cm^{-1}) is related to the CH_2 bending mode and it is a typical peak in the Raman spectrum of PVDF.[19–22] The increased I_G/I_D of PVDF-GO indicates the reduction of defects in GOs because of the interaction between PVDF and GO.

The XRD patterns of GO and PVDF-GO are shown in Fig. 1(b). A sharp peak around 10.6° in the XRD pattern of GOs is associated with the (001) inter-layer structure of GO sheets.[23,24] The XRD peaks of PVDF at 18.2° and 26.5° are related to the α phase and the peak around 20.2° is attributed to the β phase. In PVDF-GO, the intensity of the (110) peak around 20.4° significantly increases with the addition of GOs, indicating the GO-enhanced ordering microstructures of the crystalline β phase in PVDF-GO nanocomposite.[25]

B. Dielectric and pyroelectric properties of PVDF-GO nanocomposites

As shown in Fig. 2(a), the P-E loops of PVDF sample show no response to the change of temperature and very little hysteresis. The PVDF-GO sample shows totally different P-E hysteresis properties. The hysteresis loops form when the varying electric field is applied to the sample and the remnant polarization changes with the temperature. The pyroelectric coefficient of PVDF-GO nanocomposite is 2×10^{-3} $\mu C/cm^2/K$, which is much larger than that of PVDF.

To further understand the underlying mechanisms of the enhanced ferroelectric properties of PVDF-GO nanocomposites, we investigate the ferroelectric properties of GO films with a thickness of 2.0 μm. The P-E loops of GO films are shown in Fig. 2(b). The GO film is observed to possess a remnant polarization of 1.2 $\mu C/cm^2$ at 24–30 °C. Its pyroelectric coefficient is about 8×10^{-4} $\mu C/cm^2/K$. Although dipoles cannot be developed in carbon hexagonal structures, there are molecule groups such as –C = O or –C-H groups that could contribute to the formation of dipoles in GOs. As indicated by the sharp XRD peak around 10.6° (Fig. 1(b)), the GO sheets we prepared could have homogeneous sizes and inter-layer structures. It is speculated that GO films might possess spontaneous polarization since ordered

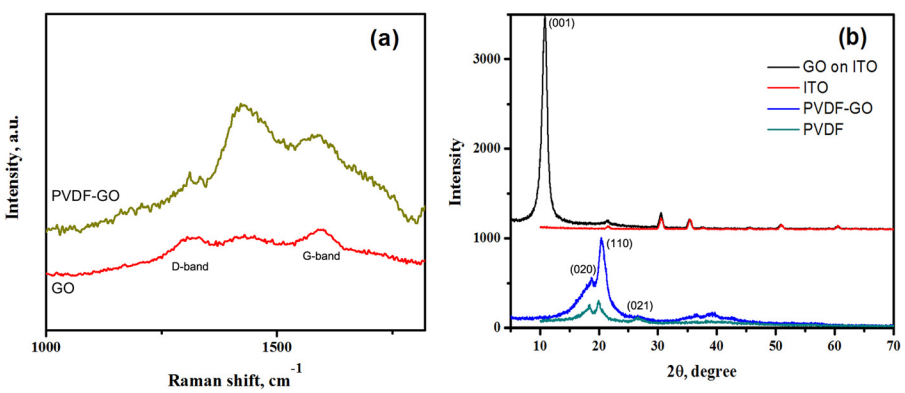

FIG. 1. (a) Raman spectra of GO and PVDF/GO nanocomposites; (b) XRD patterns of GO film on ITO substrate, PVDF and PVDF/GO nanocomposites.

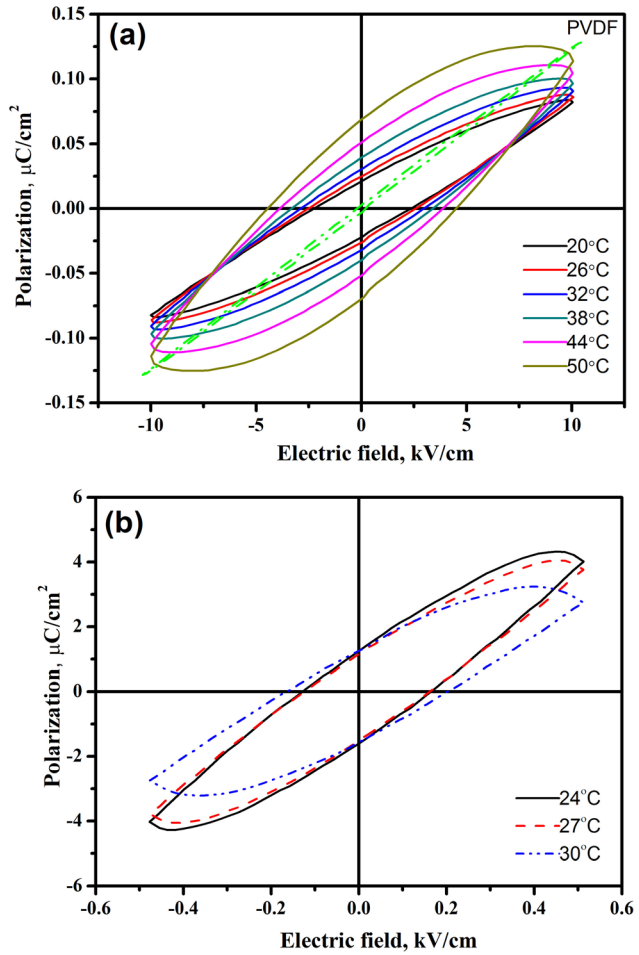

FIG. 2. (a) P-E loops of PVDF (dashed line) and PVDF/GO nanocomposites (solid lines) at different temperatures; (b) P-E loops of GO film at different temperatures.

–C = O or –C-H groups tend to form at the edges of those GO sheets. Therefore, the strong polarization of GOs may contribute to the enhanced ferroelectric property of PVDF-GO nanocomposites.

Figure 3 shows the dielectric spectra of PVDF and PVDF-GO at T = 303 K. The dielectric property of the PVDF-GO has been improved by the addition of GOs

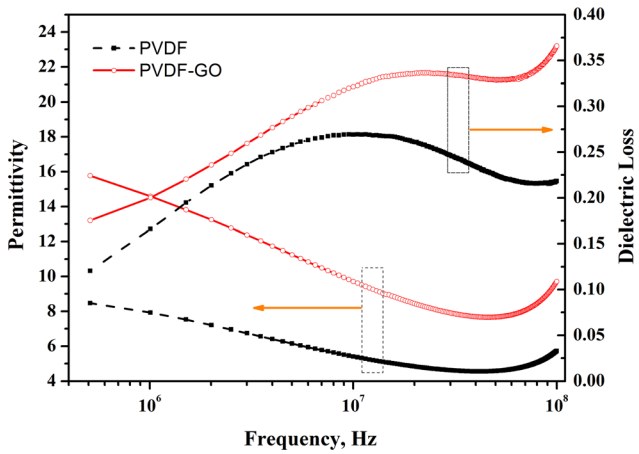

FIG. 3. Dielectric spectra of PVDF sample and the PVDF/GO nanocomposites.

especially at the 10 MHz range. In particular, the permittivity of PVDF-GO is much higher than that of PVDF. In previous investigations on the effects of nano-fillers on the permittivity of PVDF,[12] interactions among trapped charges and molecule dipoles are suggested to be responsible for the improved dielectric properties. Besides those revealed in the previous studies,[12] the effect of GO blending on the dielectric properties of PVDF could be also associated with the GO-modified structural properties of PVDF, which are discussed in Sec. III C.

C. Mechanisms of the improved properties of PVDF-GO from thermal and dynamic mechanical analyses

The improved dielectric and pyroelectric properties of PVDF-GO nanocomposites could be related with the interaction between PVDF polymer and GO sheets. The mechanisms of such interaction are revealed by thermal and dynamic mechanical analyses on the structural properties of the nanocomposites.

The differential scanning calorimetry (DSC, TA Instruments Q200) is used to characterize the effect of GO blending on the formation of crystalline phases in PVDF since the kinetics of crystallization process is closely related with the conformation and structural properties of polymers. The PVDF and PVDF-GO samples were heated above the melting point and kept for 10 min. Then, the samples were rapidly cooled with a cooling rate of 80 °C/min to a temperature between 147 and 150 °C, which was slightly lower than the melting points of the samples. The samples were held at the crystalline temperature for 30 min. Figure 4 shows the relationship between the heat flow and time, which monitors the whole crystallization process. In Figure 4, it can be found that the crystallization process in PVDF-GO starts earlier than that in PVDF and the crystallization time is much shorter than that of PVDF. The addition of GOs improves the nucleation activity of PVDF, suggesting that the PVDF chains could be affine to the dispersed GO sheets, which are nucleation sites in the melts.

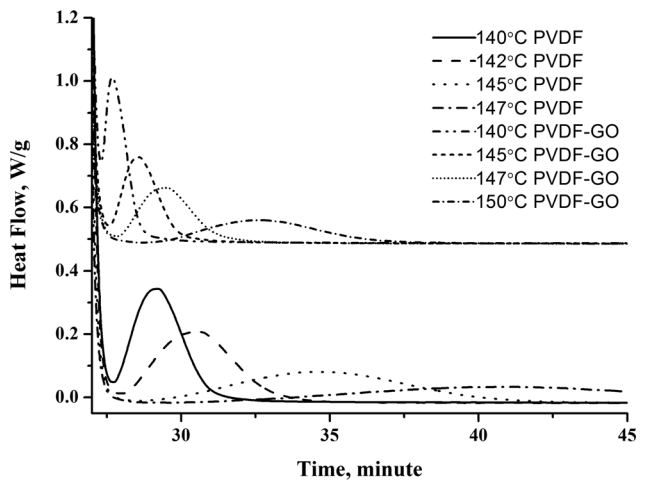

FIG. 4. Kinetics of isothermal crystallization of PVDF and PVDF/GO nanocomposites characterized by the time-dependent heat flows at various crystallization temperatures.

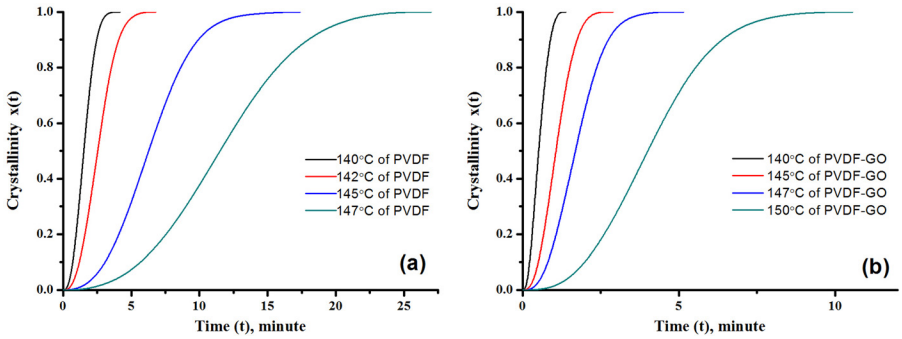

FIG. 5. The crystallization fraction x(t) of PVDF (a) and PVDF/GO nanocomposites (b) at various temperatures.

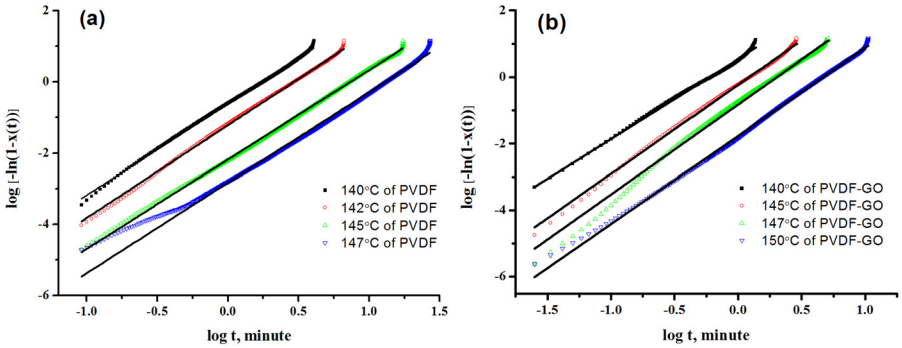

FIG. 6. The fitting of the crystallization fraction x(t) of PVDF (a) and PVDF/GO nanocomposites (b), using the Avrami equation (solid lines).

The crystallization fraction x(t) is determined using the equation[26] as follows:

$$x(\mathrm{t}) = \frac{\int_0^t \left(\frac{dH}{dt}\right) dt}{\int_0^\infty \left(\frac{dH}{dt}\right) dt}, \tag{1}$$

where H denotes the measured enthalpy of crystallization, and t represents the elapsed time of crystallization process. The time limit ∞ defines the completion of the crystallization. So the crystallinity of samples can be obtained at any time during the crystallization process.[27] Figure 5 shows x(t) at different temperatures in PVDF and PVDF-GO samples. In Figure 5, it can be found that the crystallization process of PVDF-GO is much faster than that of PVDF at the same temperature.

The features of the crystallization process are characterized by the Avrami equation as follows:[28–30]

$$\log[-\ln(1-\mathrm{x})] = \log Z + n \log t, \tag{2}$$

TABLE I. The Avrami exponent n and the crystallization rate Z of samples quenched to different crystallization temperatures T.

Samples	T (°C)	n	Z
PVDF	140.0	2.57	0.243
	142.0	2.61	0.061
	145.0	2.51	0.007
	147.0	2.54	0.001
PVDF/GO	140.0	2.40	3.490
	145.0	2.67	0.582
	147.0	2.71	0.150
	150.0	2.64	0.017

where Z denotes the crystallization rate and n represents the Avrami exponent, which determines the mechanism of nucleation and growth mode.[26] Figure 6 shows the plots of $\ln[-\ln(1-\mathrm{x}(\mathrm{t}))]$ versus $\ln t$ for isothermal crystallizations of the PVDF and PVDF-GO samples. Table I lists the results of the fittings using Eq. (2). The exponents n for PVDF and PVDF-GO are both close to 3, meaning that the crystallization of PVDF and PVDF-GO belongs to three-dimensional heterogeneous nucleation.[26] Compared with that of PVDF, the much larger rate of nucleation of PVDF-GO demonstrates that the addition of GOs significantly improve the nucleation activity of PVDF. The dispersed GOs in PVDF actually modify the microstructure of PVDF at the nano-scales and improve the ordering of microstructure of PVDF-GO. The ordered microstructure of PVDF-GO nanocomposites could result in their enhanced ferroelectric properties.

Figure 7 shows the dynamic mechanical analyses on PVDF-GO and PVDF samples. For both samples, there are internal friction (IF, Q^{-1}) peaks around $-50\,^{\circ}$C and $30\,^{\circ}$C corresponding to β and α relaxations in PVDF, respectively.[31,32] The β relaxation peak of PVDF-GO nanocomposite is broader than that of PVDF sample. Since the β peak is related with the Brownian motions of amorphous structures in PVDF,[33,34] it is suggested that the GO sheets could interact with the side chains or main chains of the amorphous phase of PVDF, increasing the viscosity of the amorphous PVDF structures. Compared to that of PVDF, the internal friction α peak in PVDF-GO is more significant and the internal friction background is reduced. The influence of GOs on the internal friction α peak implies that the ordering of microstructure of PVDF consisting of crystalline and amorphous phases could be enhanced by the addition of GOs since the α relaxation is related with the interfaces between the amorphous and crystalline structures in PVDF.

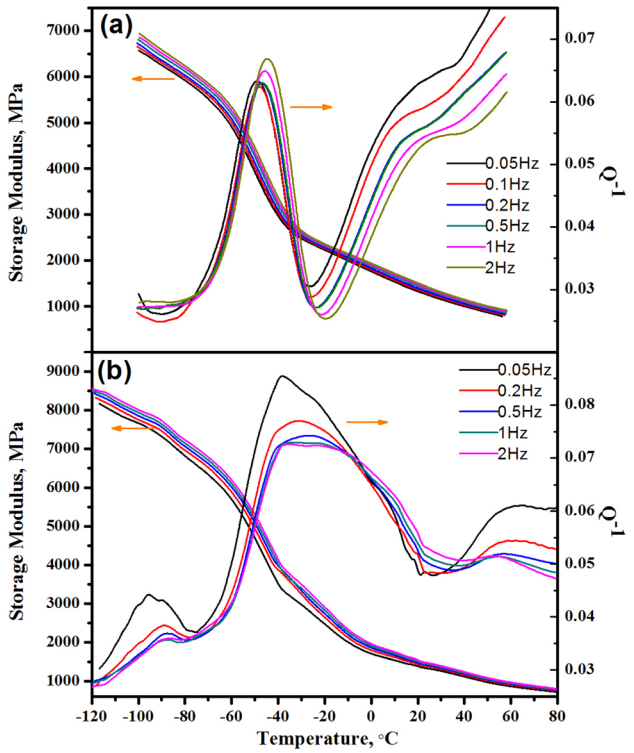

FIG. 7. The temperature-dependent internal friction and storage modulus of PVDF (a) and PVDF/GO nanocomposites (b) at different frequencies.

The IF peak for γ relaxation around $-90\,^{\circ}\mathrm{C}$ appears in PVDF-GO nanocomposite rather than in the PVDF sample. Because the γ relaxation is associated with the rotational motion of the main chains in the amorphous phase of PVDF, it is suggested the interaction between GO and the amorphous PVDF phase could result in the confined amorphous structures in PVDF. In addition, the –COH and –C = O groups in GOs could be the additional centres for the rotational relaxation, contributing to the significant γ relaxation in PVDF-GO.

The apparent activation energies E_a of β relaxation in PVDF sample and PVDF-GO nanocomposite are determined by the Vogel-Fulcher-Tammann (VFT) relation as follows:[35]

$$f = f_0 \cdot e^{-E_a/k_B(T-T_0)}, \tag{3}$$

where f is the test frequency and f_0 is the attempt frequency; $T_0 \approx T_g - 50\,\mathrm{K}$, where $T_g = -90\,^{\circ}\mathrm{C}$ is the glass transition temperature determined from the DSC.[35] As shown in Fig. 8, the activation energies of β relaxations in PVDF and PVDF-GO are found to be 0.094 eV and 0.146 eV, respectively. The enhanced apparent activation energy of β relaxation in PVDF-GO suggests that the additive GO sheets could constrain the Brownian motion of the amorphous structures in PVDF.

The apparent activation energies E_a of γ relaxation in PVDF-GO nanocomposite are determined by the Arrhenius relation as follows:

$$f = f_0 \cdot e^{-E_a/k_B T}. \tag{4}$$

As shown in the inset of Fig. 8, the activation energy of γ relaxation in PVDF-GO nanocomposite is $E_a = 0.90$ eV.

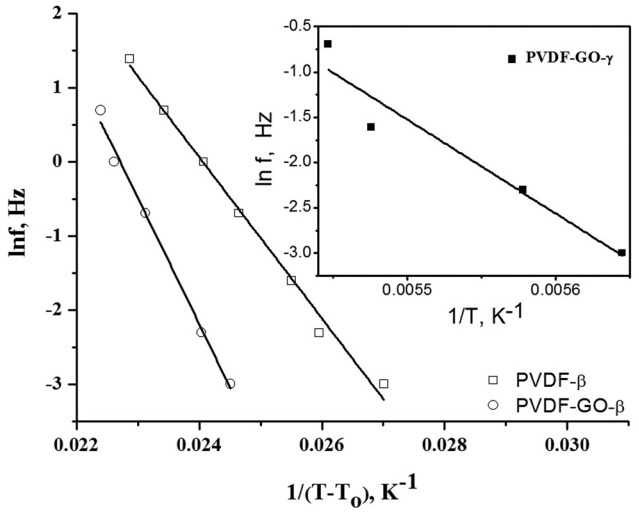

FIG. 8. Determination of the apparent activation energy of β relaxation in PVDF sample and PVDF-GO nanocomposite by the VFT relation. The inset shows the determination of the activation energy of γ relaxation in PVDF-GO nanocomposite by the Arrhenius relation.

Since this activation energy is close to that of the diffusion of oxygen (0.9–1.0 eV), it is suggested that GOs affect the structures of PVDF through the interaction between the fluorine group ($-CF_2$) of PVDF and the carbonyl groups (–C = O) of GO.

Based on the above-mentioned thermal and dynamic mechanical analyses on the structural properties of the PVDF-GO, a composite model is suggested to elucidate the enhanced dielectric and pyroelectric properties of PVDF with GO additions. Because the lateral dimensions of the GO sheets used for the preparation of PVDF-GO are several microns and the interaction between the –C = O groups in GO and the $-CF_2$ groups in PVDF is strong, PVDF-GO could be considered as a composite structure consisting of amorphous and crystalline phases of PVDF and GO sheets, which act as sharp interfaces between these two phases. The two-dimensional GO sheets not only enhance the ordering of the side chains of the crystalline PVDF structures but also confine the amorphous PVDF structures, resulting in the increased volumes of nano-regions of the crystalline PVDF phase, especially the polar crystalline β phase. In nano-sized regions, PVDF-GO exhibits larger dipolar moments compared with PVDF; in micron-sized regions, the microstructures of amorphous and crystalline phases of PVDF-GO are more ordered than those in PVDF. On the other hand, GO sheets may possess ferroelectricity. All these features could contribute to the enhanced dielectric and pyroelectric properties of PVDF-GO nanocomposites. The composite model also explains the improved shear modulus of PVDF with GO addition. Because GOs result in the increased volumes of crystalline PVDF phase, whose shear modulus is larger than that of amorphous PVDF phase, PVDF-GO has larger shear modulus than that of PVDF, as shown in Fig. 7.

IV. CONCLUSIONS

PVDF-GO nanocomposite exhibits significantly improved dielectric and pyroelectric properties compared

with those of PVDF. Based on the dynamic mechanical analyses on PVDF-GO and PVDF samples, it is demonstrated that GOs affect the structures of PVDF through the interaction between the fluorine group of PVDF and the carbonyl groups of GO. The two-dimensional GO sheets not only enhance the ordering of the side chains of the crystalline PVDF structures but also confine the amorphous PVDF structures, resulting in the increased volumes of nano-regions of the polar crystalline β phase. The enhanced ferroelectric and pyroelectric properties of PVDF-GO could be caused by the improved ordering of microstructures of PVDF due to the addition of GOs, and the individual dielectric GO sheets, which are found to possess strong polarization properties.

ACKNOWLEDGMENTS

The authors are grateful for the supports provided by the Science and Technology Innovation Commission of Shenzhen, and the Program for Eastern Scholar at Shanghai Institutions of Higher Learning.

[1]A. Linares and J. L. Acosta, "Tensile and dynamic mechanical behaviour of polymer blends based on PVDF," Eur. Polym. J. **33**(4), 467–473 (1997).
[2]T. U. Patro, M. V. Mhalgi, D. V. Khakhar, and A. Misra, "Studies on poly(vinylidene fluoride)-clay nanocomposites: Effect of different clay modifiers," Polymer **49**(16), 3486–3499 (2008).
[3]F. Bauer, "Relaxor fluorinated polymers: Novel applications and recent developments," IEEE Trans. Dielectr. Electr. Insul. **17**(4), 1106–1112 (2010).
[4]L. Liu, Y. Liu, B. Li, and J. Leng, "Theoretical investigation on polar dielectric with large electrocaloric effect as cooling devices," Appl. Phys. Lett. **99**(18), 181908-3 (2011).
[5]Q. M. Zhang, V. Bharti, and X. Zhao, "Giant electrostriction and relaxor ferroelectric behavior in electron-irradiated poly(vinylidene fluoride-trifluoroethylene) copolymer," Science **280**(5372), 2101–2104 (1998).
[6]H. Yoshida, "Structure formation of PVDF/PMMA blends studied," J. Therm. Anal. **49**(1), 101–105 (1997).
[7]F. Wang, M. Tanaka, and S. Chonan, "Development of a PVDF piezopolymer sensor for unconstrained in-sleep cardiorespiratory monitoring," J. Intell. Mater. Syst. Struct. **14**(3), 185–190 (2003).
[8]H. Luo and S. Hanagud, "PVDF film sensor and its application in damage detection," J. Aerosp. Eng. **12**(1), 23–30 (1999).
[9]H. Gu, Y. Zhao, and M. L. Wang, "A wireless smart PVDF sensor for structural health monitoring," Struct. Control Health Monitor. **12**(3-4), 329–343 (2005).
[10]A. J. Lovinger, *Developments in Crystalline Polymers—I* (Cambridge University Press, Cambridge, UK, 1982).
[11]A. Salimi and A. A. Yousefi, "Analysis method: FTIR studies of β-phase crystal formation in stretched PVDF films," Polym. Test. **22**(6), 699–704 (2003).
[12]B. J. P. Adohi, V. Laur, B. Haidar, and C. Brosseau, "Measurement of the microwave effective permittivity in tensile-strained polyvinylidene difluoride trifluoroethylene filled with graphene," Appl. Phys. Lett. **104**, 082902 (2014).
[13]M. E. Achaby, F. Z. Arrakhiz, S. Vaudreuil, E. M. Essassi, and A. Qaiss, "Piezoelectric β-polymorph formation and properties enhancement in graphene oxide-PVDF nanocomposite films," Appl. Surf. Sci. **258**(19), 7668–7677 (2012).
[14]L. He and S. C. Tjong, "A graphene oxide–polyvinylidene fluoride mixture as a precursor for fabricating thermally reduced graphene oxide–polyvinylidene fluoride composites," RSC Adv. **3**(45), 22981–22987 (2013).
[15]J. Zhang, Z. Xu, W. Mai, C. Min, B. Zhou, M. Shan, Y. Li, C. Yang, Z. Wang, and X. Qian, "Improved hydrophilicity, permeability, antifouling, and mechanical performance of PVDF composite ultrafiltration membranes tailored by oxidized low-dimensional carbon nanomaterials," J. Mater. Chem. A **1**(9), 3101–3111 (2013).
[16]Z. Han, Z. Tang, P. Li, G. Yang, Q. Zheng, and J. Yang, "Ammonia solution strengthened three-dimensional macro-porous graphene aerogel," Nanoscale **5**(21), 5462–5467 (2013).
[17]W. S. Hummers, Jr. and R. E. Offeman, "Preparation of graphitic oxide," J. Am. Chem. Soc. **80**(6), 1339 (1958).
[18]M. A. Rahman, B. C. Lee, D. T. Phan, and G. S. Chung, "Fabrication and characterization of highly efficient flexible energy harvesters using PVDF-graphene nanocomposites," Smart Mater. Struct. **22**(8), 085017 (2013).
[19]C. Zhao, X. Xu, J. Chen, and F. Yang, "Effect of graphene oxide concentration on the morphologies and antifouling properties of PVDF ultrafiltration membranes," J. Environ. Chem. Eng. **1**(3), 349–354 (2013).
[20]K. Tashiro, Y. Itoh, M. Kobayashi, and H. Tadokoro, "Polarization Raman spectra and LO-TO splitting of poly(vinylidene fluoride) crystal form I," Macromolecules **18**(12), 2600–2606 (1985).
[21]A. Jain, J. S. Kumar, S. Srikanth, V. T. Rathod, and D. R. Mahapatra, "Sensitivity of polyvinylidene fluoride films to mechanical vibration modes and impact after optimizing stretching conditions," Polym. Eng. Sci. **53**(4), 707–715 (2013).
[22]C. J. L. Constantino, A. E. Job, R. D. Simoes, J. A. Giacometti, V. Zucolotto, O. N. Oliveira, Jr., G. Gozzi, and D. L. Chinaglia, "Phase transition in poly(vinylidene fluoride) investigated with micro-Raman spectroscopy," Appl. Spectrosc. **59**(3), 275–279 (2005).
[23]D. Chen, H. Feng, and J. Li, "Graphene oxide: Preparation, functionalization, and electrochemical applications," Chem. Rev. **112**(11), 6027–6053 (2012).
[24]X. Fan, W. Peng, Y. Li, X. Li, S. Wang, G. Zhang, and F. Zhang, "Deoxygenation of exfoliated graphite oxide under alkaline conditions: A green route to graphene preparation," Adv. Mater. **20**(23), 4490–4493 (2008).
[25]M. A. Rahman and G. S. Chung, "Synthesis of PVDF-graphene nanocomposites and their properties," J. Alloys Compd. **581**, 724–730 (2013).
[26]G. Z. Papageorgiou, D. S. Achilias, D. N. Bikiaris, and G. P. Karayannidis, "Crystallization kinetics and nucleation activity of filler in polypropylene/surface-treated SiO_2 nanocomposites," Thermochim. Acta **427**(1-2), 117–128 (2005).
[27]V. Sencadas, C. M. Costa, J. L. G. Ribelles, and S. Lanceros-Mendez, "Isothermal crystallization kinetics of poly(vinylidene fluoride) in the α-phase in the scope of the avrami equation," J. Mater. Sci. **45**(5), 1328–1335 (2010).
[28]M. J. Avrami, "Kinetics of phase change I: General theory," J. Chem. Phys. **7**(12), 1103–1112 (1939).
[29]M. J. Avrami, "Kinetics of phase change II: Transformation-time relations for random distribution of nuclei," J. Chem. Phys. **8**(2), 212–224 (1940).
[30]M. J. Avrami, "Granulation, phase change, and microstructure kinetics of phase change III," J. Chem. Phys. **9**(2), 177–184 (1941).
[31]J. B. Enns and R. Simha, "Transitions in semicrystalline polymers I: Poly(vinyl fluoride) and poly(vinylidene fluoride)," J. Macromol. Sci., Part B: Phys. **13**(1), 11–24 (1977).
[32]Y. Abe, M. Kakizaki, and T. Hideshima, "Effect of the distribution of free volume on the β relaxation in poly(vinylidene fluoride)," Jpn. J. Appl. Phys., Part 1 **24**(8), 1074–1077 (1985).
[33]J. F. Mano, V. Sencadas, A. M. Costa, and S. Lanceros-Mendez, "Dynamic mechanical analysis and creep behaviour of β-PVDF films," Mater. Sci. Eng., A **370**(1-2), 336–340 (2004).
[34]A. Callens, L. Eersels, and R. D. Batist, "Low temperature internal friction on γ-irradiated polyvinylidene fluoride (PVDF)," J. Mater. Sci. **13**(9), 1887–1990 (1978).
[35]E. Ozkazanc, H. Y. Guney, T. Oskay, and E. Tarcan, "The effect of uniaxial orientation on the dielectric relaxation behavior of α-PVDF," J. Appl. Polym. Sci. **109**(6), 3878–3886 (2008).